DEEP LEARNING-BASED INTELLIGENT METHOD FOR AUTOMATIC MODULATION CLASSIFICATION IN COGNITIVE RADIOS

Gihan J. Mendis (ijm11@zips.uakron.edu), Jin Wei (jwei1@uakron.edu), and Arjuna Madanayake (arjuna@uakron.edu)

The University of Akron, Akron, Ohio, USA

ABSTRACT

This paper develop an automatic modulation classification (AMC) method for cognitive radio (CR). The proposed method employs the spectral correlation function (SCF) to generate the unique pattern signatures for each modulation scheme. Furthermore, a low-complexity binarized convolutional neural network (CNN) is designed to classify modulation schemes by recognizing the SCF-based pattern signatures. By employing the low-complexity CNN, the computationally costly 617632 floating point multiplication operations required in the conventional CNN are represented by zero computational cost no connections, simple connections, negation operations, bit-shifting operations, and bit-shifting with negation operations. This work utilizes simulated modulated signals that employed BPSK, QPSK, 2-FSK, 4-FSK, and OFDM with QPSK sub-carrier modulation schemes. The performance of the proposed method is evaluted for modulated signals with different SNRs. Furthermore, the modulation classification accuracy achieved by the proposed low-complexity CNN is compared with that achieved by the conventional CNN. The simulations section evaluates the performance of the proposed method. As shown in simulations, the accuracy of the proposed automatic modulation classification remains higher than 91% even when the SNR of the measurement environment is as low as 0 dB.

1. INTRODUCTION

With growing increase of demand frequency bands of electromagnetic spectrum using for radio frequency (RF) communication becoming a scared natural resource. Cognitive radio (CR) has attracted a lot of interest as a technique for efficiently utilizing the scarce spectrum resources [1]. In order to achieve an efficient transmission and to address the challenges of data security such as jamming, interference, and blocking, modulation schemes are being used in RF communication. BPSK, QPSK, 2FSK, 4FSK, and OFDM are some of the widely used modulation schemes that are used for encoding data on multiple carrier frequencies. Receivers of the CR systems should have the capability to automatically identify the modulation schemes used, it is an intermediate step for signal demodulation of the intelligent reciever [2]. Furthermore, detecting available modulation scheme on a carrier channel is a crucial step for spectrum sensing which is an essential function of CR systems [3, 4].

Likelihood-Based (LB) and Feature-Based (FB) approaches are the two main commonly established approaches for AMC. LB approaches provide optimal performance but require perfect knowledge of receive signals. FB approaches are sub-optimal approaches but require less prior knowledge about the received signal [2]. Most modern approaches of AMC are analytical feature-based approaches that use advanced signal processing methods to analytically derive known features. In [5], Deng *et al.* used template machine-based approach to classify multi-level amplitude phase shift keying (MAPSK) signals. In [6], Wu *et al.* suggest using analysis of higher orders statistics to engineered features for modulation detection.

Deep learning methods are artificial neural network (ANN) based machine learning techniques that have multiple layer hierarchies of ANNs. These techniques are more effective in extracting hierarchical features from raw data [7]. Deep learning methods have been used for pattern recognition in various application areas [8–12]. In our previous work, we proposed an automated modulation classification (AMC) method with a signal processing mechanism that uses spectral correlation function (SCF) to generate noise-resilient and distinguishable 2-D signature patterns and deep belief network (DBN) based classifier for classification of modulation schemes [13]. Convolutional neural networks (CNNs) are one of the most successful deep learning techniques inspired by the neuron arrangement of the visual cortex of mammals [14]. CNN-based methods are widely used for image classification tasks including radar signature analysis [15–18], In this paper, we leverage CNN as the deep learning-based classification method for the AMC.

The main challenge of implementing deep learning methods is the high computation-complexity that increases the power and area cost of digital implementations for deep learning based classifiers. High computation-complexity is a result of the high number of floating-point multiplications operations. In our previous work, we proposed a multiplierless low-complexity DBN with direct mapping to binary logic circuits to use as the classification technique for AMC [19]. In this work, we design a multiplierless CNN-based classifier for classification of SCF patterns of modulation methods. In [20], Lin *et al.* proposed a binarization method for backpropagation algorithm which produces binary weights $\{-1, 0, 1\}$. In this paper, we exploit this method to realize the multiplierless low-complexity CNN.

In the following section, we provide an overview of the proposed system. Sections 3 and 4 briefly discuss SCF pattern generation and the low-complexity CNN, respectively. The simulation of modulated signals, implementation of proposed low-complexity CNN for modulation classification, and the summary results obtained are shown in Section 6. In Section 7, the conclusions and future work are presented.

2. OVERVIEW

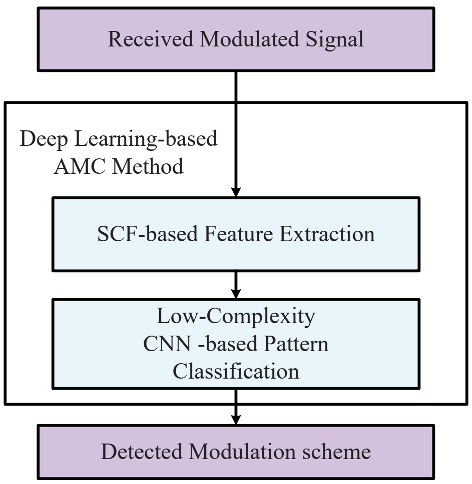

Figure 1: Overview of the proposed system.

As shown in Fig. 1, the proposed deep learning-based AMC method contains a spectral correlation function (SCF)-based feature extraction method followed by the low-complexity CNN-based pattern classifier, which classifies the generated SCF patterns to identify the embodied modulation scheme of the received signal.

3. SCF SIGNATURE PATTERNS

Cyclic Autocorrelation Function (CAF) is defined to quantize the amount of correlation between different frequency shifted versions of a given signal and represent the fundamental parameters of their second order periodicity [21]. CAF is calculated as follows:

$$R_x^{\alpha}[l] = \left[\lim_{N \to \infty} \frac{1}{2N+1} \sum_{n=-N}^{N} x[n]x^*[n-l]e^{-j2\pi\alpha n} \right] e^{-j\pi\alpha l} \tag{1}$$

Where $x[\cdot]$ is the given signal and $\alpha = m/T_0$ is the cyclic frequency, T_0 is the process period, and m is an integer. Spectral correlation function (SCF) is the Fourier transform of CAF, which is described in the following equation.

$$S_x^{\alpha}[f] = \sum_{l=-\infty}^{\infty} R_x^{\alpha}[l]e^{-j2\pi fl} \tag{2}$$

Table 1: The floating-point multiplication operations required in CNN.

Layer	Floating point Multiplications
Convolution layer 1	$24 \times 24 \times 5 \times 5 \times 32 = 460800$
Convolution layer 2	$12 \times 12 \times 5 \times 5 \times 32 = 115200$
Convolution layer 3	$6 \times 6 \times 2 \times 2 \times 32 = 4608$
Fully connected ReLU	$1152 \times 32 = 36864$
Fully connected softmax	$32 \times 5 = 160$
The Number of Required Multiplications	617632

Where f the temporal frequency of the given signal.

Modulated signals contain 2nd order periodic statistical features associated with the corresponding modulation scheme. 2-D order features unique to each modulation scheme can be extracted from the SCF of the modulated signal [21]. In this work, we use SCF pattern classify modulation schemes such as FSK, BPSK, QPSK, and OFDM. However, to identify higher order modulations, such as 16QAM and 64QAM, higher order methods need to be used [22]. Another advantage of using the SCF patterns is the resilience to stationary impairments such as additive white Gaussian noise (AWGN) because the SCF suppresses stationary features [21].

4. LOW-COMPLEXITY CONVOLUTIONAL NEURAL NETWORK

As shown in the Fig. 2, the CNN designed in our work consists of 3 convolution layers, 2 pooling layers, a fully connected layer with rectifier linear units (ReLU), and a softmax-based output layer. The inputs to the CNN are 2D images having the size of 24×24. The first convolution layer evaluates 32 features with 5×5 kernel size. Maximum pooling is performed after the first convolution layer with the kernel size of 2×2, which reduces the image size to 12×12. The second convolution layer evaluates 32 features with 5×5 kernel size along with 2 maximum pooling, which reduces the size of the image to 6×6. The third convolution layer evaluates 32 features with 2×2 kernel size. The outputs of the 32 kernels of the third convolution layer are reshaped and combined to form a vector of the size $6 \times 6 \times 32 = 1152$. A fully connected layer with 1024 ReLU units is added on top along with a softmax layer for classification.

If the weights of the convolution layers and fully connected layers remain as floating-point numbers, the total number of floating point multiplication operations required to perform in a single iteration of testing is shown in Table 1, where we assume the number of class labels as 5. Since floating point multiplication is computationally expensive in digital logic and the number of the total multiplications required for the CNN is very high, the deployments of the above CNN becomes a hardware-expensive task. By modifying the backpropagation algorithm of the CNN as shown in Table 2, we replace the floating-point weights of the CNN by using five possible values $-2^p, -1, 0, 1, 2^p$, where

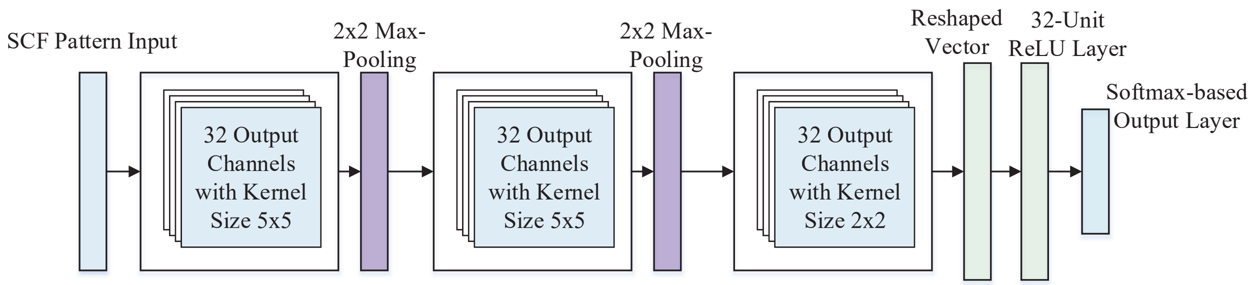

Figure 2: The structure of CNN.

p is a positive integer. By doing so, we reduce the hardware-expensive floating-point multiplications to the operations that are much less costly in the digital hardware as shown in Table 3.

5. SIMULATION RESULTS

In this section, we evaluate our proposed method. Furthermore, we also compare the accuracy of our proposed low-complexity CNN, that is the essential component of our method, with that achieved by the conventional CNN.

Simulation of Modulated Signals

We simulate the modulated signals with different modulations schemes using MATLAB/Simulink software. The modulation schemes used in this work are ASK, 2FSK, 4FSK, BPSK, QPSK, and OFDM with BPSK modulated sub-carriers. For all simulated signals, the carrier frequency is selected as 1 kHz and the symbol rate is chosen to be 100 Hz. The amplitudes of the signals are normalized to the range [0, 1]. For simulation of BPSK and 2-FSK modulated signal, a data stream of 256 symbols with binary symbols in random order is used. In 2-FSK modulation scheme, the two frequencies used for modulation are 100 Hz and 160 Hz. For simulation of QPSK and 4-FSK modulated signal, a data stream of 256 symbols with 4 symbols in random order is used. In 4-FSK modulation scheme, the four frequencies used for modulation are 100 Hz, 120 Hz, 140 Hz, and 160 Hz. For the simulation of OFDM, 256 data random data stream is used with 4 symbols. OFDM system simulated contains 128 QPSK modulated sub-carriers.

In order to study the resilience of proposed method in fading channels, we added additive white Gaussian noise (AWGN) to simulated modulated signals. Therefore, the signals are simulated with a range of SNR 0 - 5 dB. SCF patterns of simulated modulated signals are generated using a MATLAB Communications System Toolbox functions [23]. SCF patterns generated for simulated BPSK, QPSK, 2-FSK, 4-FSK, and OFDM with QPSK sub-carriers modulation schemes with SNR 5 dB are shown in Figs. 3, 4, 5, 6, and 7, respectively. Figure 8 shows the 2D projection of the SCF patterns for the simulated modulation schemes when SNR is 5 dB.

Table 2: The training algorithm for updating our low-complexity CNN.

Operators and functions:
$.\geq$: the elementwise more than or equal comparison of two matrices.
$.\times$: the elementwise multiplication of two matrices.
$y = sign(x)$: if $x < 0$, $y = -1$, else $y = 1$.
$y = absolute(x)$: if $x < 0$, $y = -x$, else $y = x$.
$\mathbf{Y} = rand(\mathbf{X})$: randomly assigns $y_{ij} \in [0, 1]$ and $dim(\mathbf{Y}) = dim(\mathbf{X})$.
$y = cast(x)$: if $x = true$, $y = 1$, else $y = 0$.
$\mathbf{W} = backprop(\mathbf{W}, f)$: applies the gradient descent based backpropagation algorithm to fine-tune the weight matrix $\mathbf{W}$, where f is a batch of training data.
$f = nextbatch(\mathbf{F}, batchsize)$: returns the next batch of training data according to batch size, where $\mathbf{F}$ is the training data set.
$\mathbf{W_c} = clipping(\mathbf{W}, L)$: clips the element values of weight matrix $\mathbf{W}$ to be in the range $[-L, L]$ where L is a predetermined scalar.

Inputs: L-clipping level, $\mathbf{W}$-initial weight matrix , $\mathbf{F}$-training data, $\mathbf{T}$-labels corresponding to training data, N-number of training iterations.

Output: $\mathbf{W_b}$-binarized weight matrix ($w_{ij} \in \{-1, 0, 1\}$)

Steps:
For $epoch \leqslant N$
  $f = nextbatch(\mathbf{F}, 50)$
  $\mathbf{W} = backprop(\mathbf{W}, f)$
  If $(mode(epoch, 100) = 0)$
    $\mathbf{W_c} = clipping(\mathbf{W}, L)$
    $\mathbf{S} = sign(\mathbf{W_c})$
    $\mathbf{P} = absolute(\mathbf{W_c})/L$
    $\mathbf{T} = \mathbf{P}. \geq rand(\mathbf{P})$
    $\mathbf{W_b} = cast(\mathbf{T}). \times \mathbf{S}$
  End
End

Table 3: Digital logic mapping of multiplications with low-complexity weights.

Weight Value	Mapping
0	No connection
1	Connection
-1	Negation
2^p	Right shift by p bits
-2^p	Right shift by p bits and negation

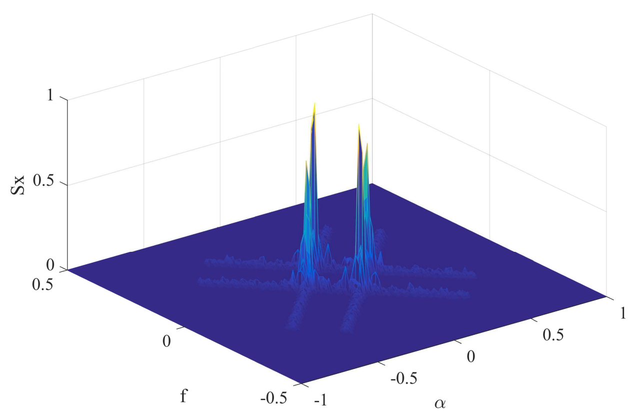

Figure 3: SCF pattern of simulated BPSK modulated signal: SNR of the simulated signal is 5 dB.

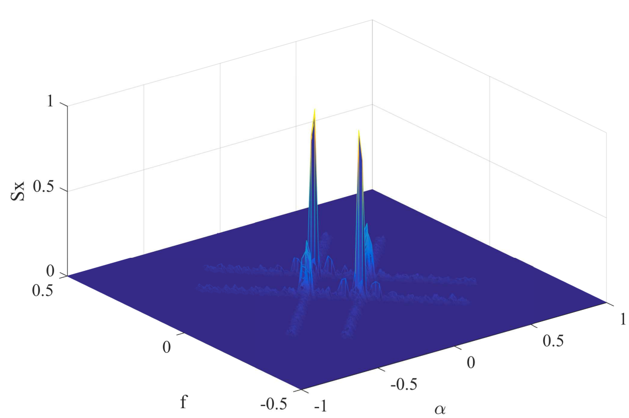

Figure 4: SCF pattern of simulated QPSK modulated signal: SNR of the simulated signal is 5 dB.

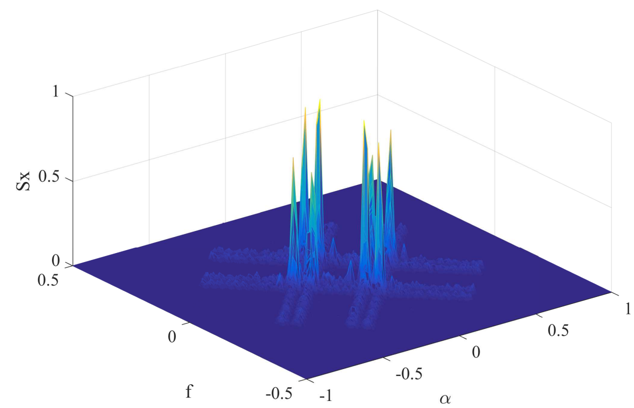

Figure 5: SCF pattern of simulated 2-FSK modulated signal: SNR of the simulated signal is 5 dB.

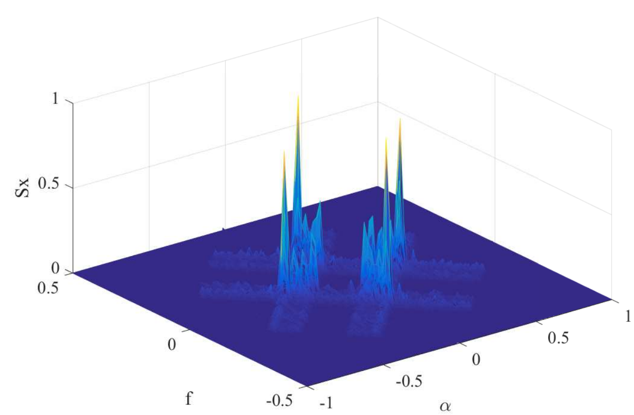

Figure 6: SCF pattern of simulated 4-FSK modulated signal: SNR of the simulated signal is 5 dB.

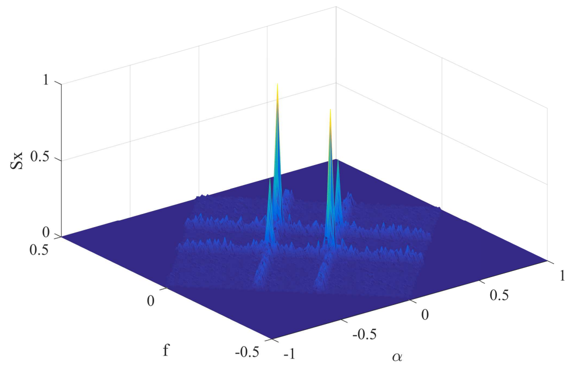

Figure 7: SCF pattern of simulated OFDM modulated signal: SNR of the simulated signal is 5 dB.

Pre-Processing and Training

The gray-scale images of the SCF patterns are resized to be 48×48 images. Fast Fourier transform (FFT) based method is used for image scaling. A 2-dimensional (2D) FFT operation is implemented on the original grayscale images and a 48×48 pixel square is selected from the center of the FFT transformed image. Then inverse 2D FFT is performed to achieve the scaled down image. By doing so, high-frequency components of the original image are filtered out, and thus high-frequency noise is removed from the scaled down image. Considering the symmetry of the patterns, a quarter of the pixels from the resized images is used as the input for the low-complexity CNN classifier. Therefore, the input size of the low-complexity CNN is 24×24.

The low-complexity CNN is trained using data that includes 400 of 2000 patterns corresponding to each modulation scheme which contained SCF patterns generated for signals with different SNR levels. As a comparison, a conventional CNN, which has the same structure but uses floating-point accurate weights, are also trained with the same 2000 training data. Another data set containing 250 patterns from each SNR for each modulation scheme is used to evaluate the performances of the CNNs. The classifiers based on low-complexity and conventional CNNs are implemented using TensorFlow APIs [24]. In the simulation, we set the number of iterations as 2000 and the batch size to be 20. At each 100th iteration of backpropagation training, binarization is performed for the low-complexity CNN. The simulation results are illustrated in the following subsection.

Results

The classification accuracy low-complexity CNNs and conventional CNN as the SNR of the modulated signal changes from 0 to 5 dB are shown in Figs. 9 and 10, respectively.

From Figs. 9 and 10, we can observe that the classification accuracy reduces as the SNR decreases from 5 to 0 dB. For conventional CNN, classification accuracy is above 98% for all modulation schemes except BPSK. For BPSK modulation scheme, classification accuracy observed from conventional CNN is 92%. For our low-complexity CNN, the classification accuracy is above 97% for all modulation schemes except BPSK. For BPSK modulation scheme, the classification accuracy observed for low-complexity CNN is 91.2%. Therefore, based on the simulation results, we can observe that our low-complexity CNN achieves comparable accuracy in classification of modulation schemes compared with that achieved by conventional CNN. Furthermore, our proposed CNN outperforms the conventional CNN in low computational complexity. Overall, our proposed CNN achieves a good tradeoff between the performance and the computational complexity.

6. CONCLUSION

This paper proposes a deep learning-based cognitive radar system for automatic modulation classification in cognitive radio by using SCF function and low-complexity CNN method. The noise resilient SCF generate unique signature patterns for each modulation scheme and the low-complexity CNN is designed to classify the patterns. Our proposed low-complexity CNN has the advantage of containing no multipliers while a conventional CNN with the same structure requires performing 617632 floating-point multiplication operations. As illustrated in the simulation results, our proposed low-complexity CNN method achieve comparable accuracy compared with conventional CNN. As future work, we plan to study the possibility of SCF base feature extraction for higher order modulation schemes and apply the proposed method for real-time detection of modulations in experimentally captured signals.

REFERENCES

[1] S. Haykin, "Cognitive radio: brain-empowered wireless communications," *IEEE Journal on Selected Areas in Communications*, vol. 23, no. 2, pp. 201–220, Feb 2005.

[2] O. A. Dobre, A. Abdi, Y. Bar-Ness, and W. Su, "Survey of automatic modulation classification techniques: classical approaches and new trends," *IET communications*, vol. 1, no. 2, pp. 137–156, 2007.

[3] W.-Y. Lee and I. F. Akyildiz, "Optimal spectrum sensing framework for cognitive radio networks," *IEEE Transactions on wireless communications*, vol. 7, no. 10, 2008.

[4] C.-T. Chou, H. Kim, K. G. Shin *et al.*, "What and how much to gain by spectrum agility?" *IEEE Journal on Selected Areas in Communications*, vol. 25, no. 3, 2007.

[5] Y. c. Deng and Z. g. Wang, "Modulation recognition of mapsk signals using template matching," *Electronics Letters*, vol. 50, no. 25, pp. 1986–1988, 2014.

[6] H.-C. Wu, M. Saquib, and Z. Yun, "Novel automatic modulation classification using cumulant features for communications via multipath channels," *IEEE Transactions on Wireless Communications*, vol. 7, no. 8, 2008.

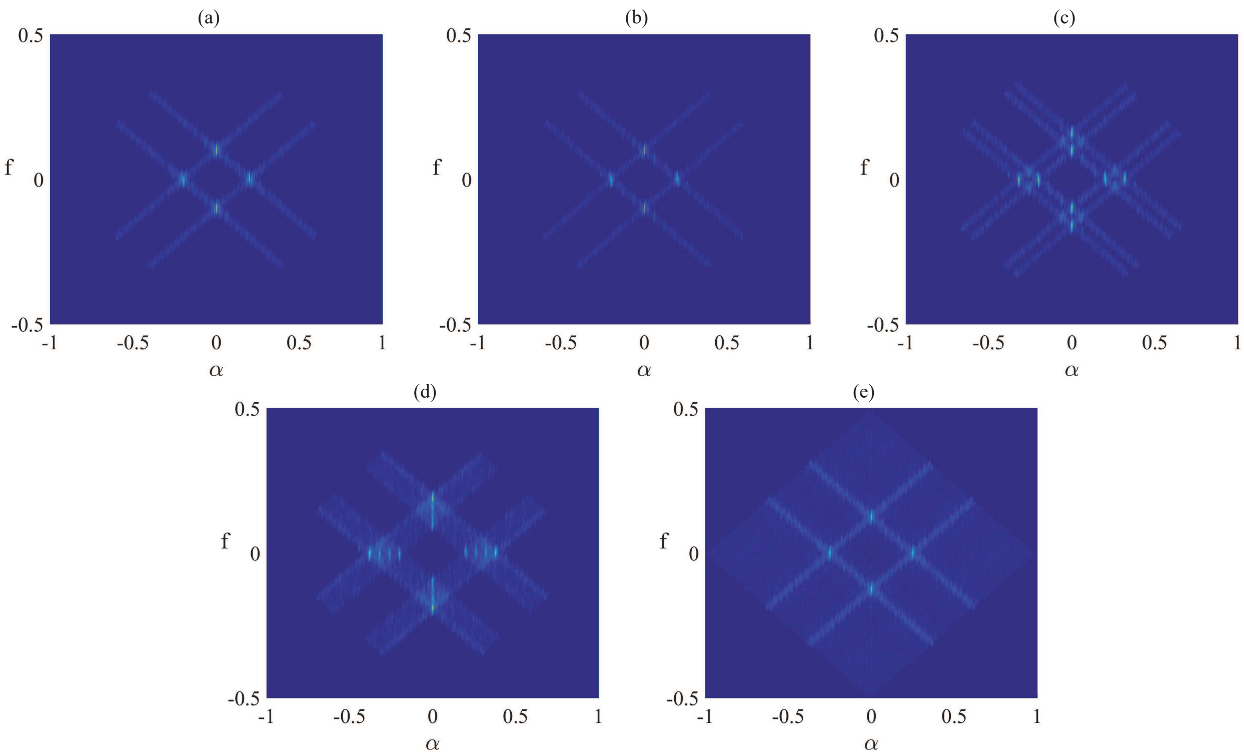

Figure 8: 2D SCF patterns of simulated modulated signal (a) BPSK; (b) QPSK; (c) 2-FSK; (d) 4-FSK; (e) OFDM with BPSK sub-carrier modulation: SNR of the simulated signals is 5 dB.

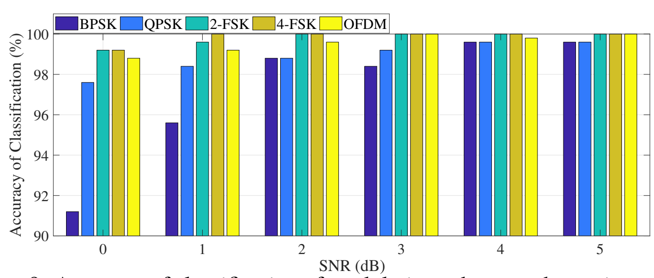

Figure 9: Accuracy of classification of modulation schemes when using low-complexity CNN as the SNR of modulated signal varies from 0 to 5 dB.

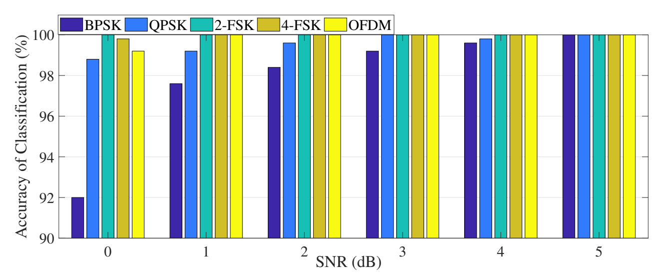

Figure 10: Accuracy of classification of modulation schemes when using conventional CNN as the SNR of modulated signal varies from 0 to 5 dB.

[7] Y. LeCun, Y. Bengio, and G. Hinton, "Deep learning," *Nature*, vol. 521, no. 7553, pp. 436–444, 2015.

[8] G. E. Dahl, D. Yu, L. Deng, and A. Acero, "Context-dependent pre-trained deep neural networks for large-vocabulary speech recognition," *IEEE Transactions on audio, speech, and language processing*, vol. 20, no. 1, pp. 30–42, 2012.

[9] G. Hinton, L. Deng, D. Yu, G. E. Dahl, A.-r. Mohamed, N. Jaitly, A. Senior, V. Vanhoucke, P. Nguyen, T. N. Sainath *et al.*, "Deep neural networks for acoustic modeling in speech recognition: The shared views of four research groups," *IEEE Signal Processing Magazine*, vol. 29, no. 6, pp. 82–97, 2012.

[10] A. Venkataraman, "Deep learning algorithms based text classifier," in *2016 2nd International Conference on Applied and Theoretical Computing and Communication Technology (iCATccT)*, July 2016, pp. 220–224.

[11] Q. Weng, Z. Mao, J. Lin, and W. Guo, "Land-use classification via extreme learning classifier based on deep convolutional features," *IEEE Geoscience and Remote Sensing Letters*, vol. 14, no. 5, pp. 704–708, May 2017.

[12] K. Matsumoto, Y. Tajima, R. Saito, M. Nakata, H. Sato, T. Kovacs, and K. Takadama, "Learning classifier system with deep autoencoder," in *2016 IEEE Congress on Evolutionary Computation (CEC)*, July 2016, pp. 4739–4746.

[13] G. J. Mendis, J. Wei, and A. Madanayake, "Deep learning-based automated modulation classification for cognitive radio," in *Communication Systems (ICCS), 2016 IEEE International Conference on*. IEEE, 2016, pp. 1–6.

[14] D. D. Cox and T. Dean, "Neural networks and neuroscience-inspired computer vision," *Current Biology*, vol. 24, no. 18, pp. R921–R929, 2014.

[15] S. Lawrence, C. L. Giles, A. C. Tsoi, and A. D. Back, "Face recognition: a convolutional neural-network approach," *IEEE Transactions on Neural Networks*, vol. 8, no. 1, pp. 98–113, Jan 1997.

[16] A. Krizhevsky, I. Sutskever, and G. E. Hinton, "ImageNet classification with deep convolutional neural networks," in *Advances in Neural Information Processing Systems 25*, F. Pereira, C. J. C. Burges, L. Bottou, and K. Q. Weinberger, Eds. Curran Associates, Inc., 2012, pp. 1097–1105. [Online]. Available: http://papers.nips.cc/paper/4824-imagenet-classification-with-deep-convolutional-neural-networks.pdf

[17] J. Yang, Y. Zhao, J. C. W. Chan, and C. Yi, "Hyperspectral image classification using two-channel deep convolutional neural network," in *2016 IEEE International Geoscience and Remote Sensing Symposium (IGARSS)*, July 2016, pp. 5079–5082.

[18] Y. Kim and T. Moon, "Human detection and activity classification based on micro-Doppler signatures using deep convolutional neural networks," *IEEE Geoscience and Remote Sensing Letters*, vol. 13, no. 1, pp. 8–12, Jan 2016.

[19] G. J. Mendis, J. Wei, and A. Madanayake, "Deep belief network for automated modulation classification in cognitive radio," in *Cognitive Communications for Aerospace Applications Workshop (CCAA), 2017*. IEEE, 2017, pp. 1–5.

[20] Z. Lin, M. Courbariaux, R. Memisevic, and Y. Bengio, "Neural networks with few multiplications," *arXiv preprint arXiv:1510.03009*, 2015.

[21] W. A. Gardner, A. Napolitano, and L. Paura, "Cyclostationarity: Half a century of research," *Signal processing*, vol. 86, no. 4, pp. 639–697, 2006.

[22] A. Fehske, J. Gaeddert, and J. H. Reed, "A new approach to signal classification using spectral correlation and neural networks," in *New Frontiers in Dynamic Spectrum Access Networks, 2005. DySPAN 2005. 2005 First IEEE International Symposium on*. IEEE, 2005, pp. 144–150.

[23] "P25 spectrum sensing with synthesized and captured data," https://www.mathworks.com/help/comm/examples/p25-spectrum-sensing-with-synthesized-and-captured-data.html.

[24] M. Abadi, A. Agarwal, P. Barham, E. Brevdo, Z. Chen, C. Citro, G. S. Corrado, A. Davis, J. Dean, M. Devin *et al.*, "Tensorflow: Large-scale machine learning on heterogeneous distributed systems," *arXiv preprint arXiv:1603.04467*, 2016.